THE ASTROPHYSICAL JOURNAL, 433:357–360, 1994 September 20

GRAVITOMAGNETICS IN STATIONARY MEDIA

E. WOYK
Astronomical Institute (Chvojková), Czech Academy of Sciences, Boční II, 1, 140 00 Praha 4, Spořilov, Czech Republic
Received 1993 August 20; accepted 1994 March 28

ABSTRACT

A new gravitomagnetic theory is used to investigate the trajectories of charged particles, spiraling in extended gravity and magnetic fields. In undisturbed atmospheres, collisions result in a slow top-trapping of ions with sufficient energies to escape that explains the extremely high temperature in coronas, radiation belts, etc. In disturbed media, force-free streams occur (merely due to the change of the pitch angle variation) that explain the occurrence and disappearance of auroae or the surprising flare effect, that is, the spiraling through a "magnetic hole."

Subject headings: acceleration of particles — gravitation — MHD

1. INTRODUCTION

In order to simplify the theory of the effect of the magnetic field upon cosmic atmospheres, an attempt has been made to develop a less complicated theory: from the equation of motion of charged particles spiraling in extended gravity and magnetic fields, I develop a formula valid for any possible path. It yields qualitative information about phenomena occurring in cosmic atmospheres. Each path is defined by only two basic parameters: one describing the effect of gravity and velocity, the other describing the magnetic field.

2. DERIVATION OF THE BASIC GRAVITOMAGNETIC PARTICLE PATH FORMULA

Trajectories of charged particles, spiraling in very extended magnetic and gravity fields, are explicitly defined by

$$\sin i = v_\perp / v \; ; \tag{1}$$

i is the pitch angle and v is the particle velocity (constant in a gravity-free medium); $v_\perp$ is its component perpendicular to H. Each point of the field line is defined by its distance r from the gravity center; at the path end, the magnetic mirror $r_H = r_{(1)}$, the ion circles, perpendicular to the field H before reflecting back again. Since all formulae are dimensionless one replaces r by

$$\rho = r / r_{(1)} \; , \tag{2}$$

where $r_{(1)}$ is the radius at which $i = 90°$, from which the particle is reflected back. Two levels $r_{(1)}$ can occur: r_H and r_g corresponding to $\rho_{(1)}$ and $\rho_{(2)}$.

Instead of the well-known magnetic dipole-field one employs the dipole-like field

$$H / H_{(1)} = \rho^{-3} \; .$$

The latitude dependence of H, which varies between 1 and 2, is negligible with respect to the altitude dependence, which is often between $H_{(1)}$ and $10^{10} H_{(1)}$ in stationary undisturbed regions. If the magnetic field lines are disturbed one applies

$$H / H_{(1)} = \rho^{-n} \; . \tag{3}$$

Alfvén's invariant

$$H / v_\perp^2 = \text{const}$$

and equation (3) yield the formula for the velocity component $v_\perp$ of equation (1):

$$v_\perp / v_{\perp(1)} = \rho^{-n/2} \; . \tag{4}$$

In order to obtain the velocity v, the equation of motion must be considered:

$$m\ddot{\boldsymbol{r}} = e\dot{\boldsymbol{r}} \times H - (GMm / r^3)\boldsymbol{r} \; , \tag{5}$$

where

$$2GM / r = v_{\text{esc}}^2 \; , \tag{6}$$

and the ratio v_{esc} / v defines E and the basic path parameter $E_{(1)}$:

$$\left.\begin{aligned} (v_{\text{esc}} / v)^2 = E &= (2GM / r v^2) \\ E_{(1)} &= 2GM / r_{(1)} v_{(1)}^2 \end{aligned}\right\} \; . \tag{7}$$

The magnetic parameter n and the velocity parameter $E_{(1)}$ are capable of describing any possible particle path—even in very distorted magnetic fields; see Figure 1.

The vector product of $\boldsymbol{r}$ with equation (5) and the scalar product of $\dot{\boldsymbol{r}}$ with equation (5) verify the above statement that the magnetic and gravity effects are independent of each other. The scalar product (with $\dot{\boldsymbol{r}}$) yields, following integration,

$$v^2 - v_{(1)}^2 = v_{\text{esc},(1)}^2 / \rho - v_{\text{esc},(1)}^2$$

or

$$v / v_{(1)} = [E_{(1)} / \rho + (1 - E_{(1)})]^{1/2} \; . \tag{8}$$

After having introduced equations (4) and (8) into equation (1) we obtain the basic path formula, $i(\rho)$,

$$\sin i = [E_{(1)} \rho^{n-1} + (1 - E_{(1)}) \rho^n]^{-1/2} \tag{9}$$

(note: $v(1)$ equals $v_{\perp,(1)}$!) We may rewrite equation (9) in the form of a determinant:

$$\begin{vmatrix} E_{(1)} \, , & E_{(1)} - 1 \\ \rho^n \, , & \rho^{n-1} \end{vmatrix} \cdot \sin^2 i = 1 \; . \tag{10}$$

The path formula (10) is dimensionless, and it contains no differential expression. The two parameters, $E_{(1)}$ and n, are able to describe any ion trajectory under most disturbed conditions as illustrated in Figure 1. In disturbed atmospheres one simply applies another value of the magnetic parameter n.

Some additional path formulae, deduced from equations (10) or (9), respectively, will only briefly be mentioned.

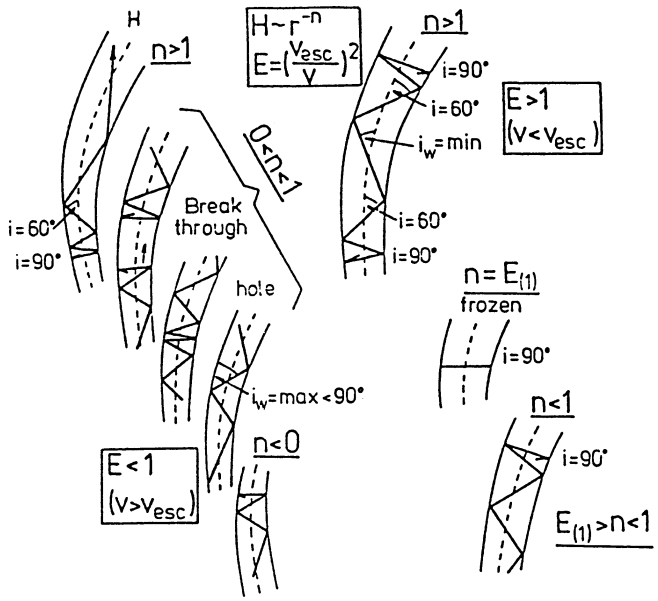

FIG. 1.—Possible ion trajectories for various n and $E_{(1)}$. *Top*: $n > 1$, i.e., H decreases with altitude (including the dipole-like field); *bottom*: $n < 0$, i.e., H grows with ρ in a disturbed region; *left*: superescape ions—$E_{(1)} < 1$, the left center refers to the case $0 < n < 1$; *right*: underescape ions—$E_{(1)} > 1$.

Underescape paths, $v < v_{esc}$, $E > 1$, and some singular superescape paths, $v > v_{esc}$, have two limits: the magnetic mirror $r_{(1)} = r_H$ and the upper path end, due to gravity, $r_{(2)} = r_g$. Thus, there may be two different values for the limiting value of r: one value refers to $\rho_{(1)} = \rho_H$, the other one to $\rho_{(2)} = \rho_g$. Here r_g or ρ_g are the uppermost altitude an ion spiraling with a cyclotron frequency ω and tube gyroradius $R \propto \rho^{n/2}$ (or velocity v) can attain in the gravity field.

In undisturbed stationary atmospheres where $n = 3$ one simply divides equation (9) by $(\rho - 1)$ and gets

$$\rho_{(2)} = \frac{1 + 2\sqrt{E_{(1)} - 0.75}}{2(E_{(1)} - 1)} . \tag{11}$$

E defines the velocity v at an arbitrary point r, or ρ, respectively; $E_{(1)}$ defines each individual path. The two equations (7) yield

$$E_{(1)} = \frac{E\rho}{E\rho - (E - 1)} \tag{12}$$

and

$$E = \frac{E_{(1)}}{E_{(1)} - (E_{(1)} - 1)\rho} . \tag{13}$$

Between collisions each ion spirals as if it would attain the level $\rho_{(1)}$ with the energy ratio $E_{(1)}$.

Between $\rho_{(1)}$ and $\rho_{(2)}$, where $i = 90°$, there must exist a level ρ_W at which i = minimum. This level follows from equations (9) or (10) applying $di/d\rho = 0$ and using equation (7). It is characterized by

$$E_W = n , \tag{14}$$

or

$$v_W = v_{esc}/\sqrt{n} . \tag{15}$$

Further,

$$\rho_W = \frac{E_{(1)}}{n} \frac{n - 1}{E_{(1)} - 1} \tag{16}$$

and

$$\sin i_W = \left(\frac{E_{(1)} - 1}{n - 1}\right)^{(n-1)/2} \left(\frac{E_{(1)}}{n}\right)^{-n/2} \tag{17}$$

3. SPECIFIC GRAVITOMAGNETIC PROPERTIES

The real path of each charged particle—freely spiraling in extended cosmic magnetic fields between collisions—is always part of the path (eq. [10]) derived for collisionless media.

A collision determines new values of E and i (of velocity and direction) at the "altitude" r. The path is found from equations (10) and (12).

In an undisturbed, stationary atmosphere $n = 3$. The field is dipole-like. Charged particles with $v > v_{esc}$ (top of Fig. 2) have only one path end with $i = 90°$, the well-known magnetic mirror r_H at the bottom of the path. When they rise their pitch angle i diminishes to $i = 0°$ (theoretically at $r = \infty$). When an ion begins its path at a level r the altitude distance, passed through between two collisions, is longer in the mean if the ion has spiraled away from the path end $\rho = 1$ than if it approaches $\rho = 1$ where $v_{\|} = 0$. This explains the extremely high temperature in stellar coronae, planetary radiation belts, etc.

Underescape charged particles ($v < v_{esc}$) possess an upper path end, r_g, which is due to gravity and at which $i = 90°$, besides the magnetic mirror r_H, due to H. They are perpetually reflected up and down. Their pitch angle i is minimum at the level r_W given by equations (14)–(17).

Figure 1 also presents the types of particle paths found for $n \neq 3$: In disturbed cosmic atmospheres, the magnetic parameter n continuously varies along H. The path must now be separated into smaller segments in which n can already be regarded constant, and equations (10) and (12) applied for determining the whole path. The calculation may readily be performed numerically.

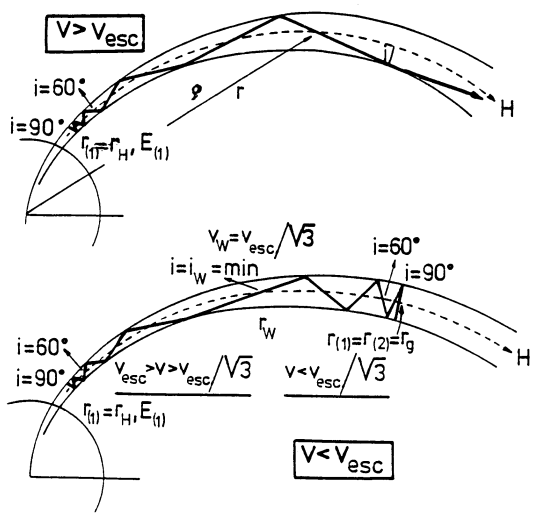

FIG. 2.—Trajectories of the top of Fig. 1 valid in undisturbed dipole-like atmospheres, $n = 3$. *Top*: superescape ions, $E_{(1)} < 1$; *bottom*: underescape ones, $E_{(1)} > 1$, with two path ends.

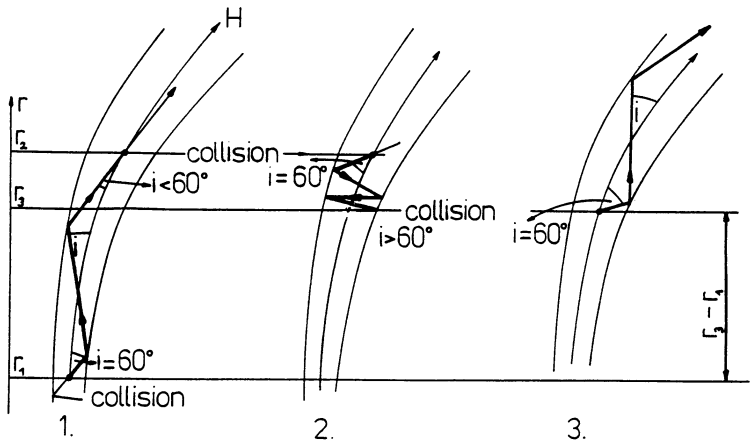

FIG. 3.—Top-trapping of a superscape charged particle. Each odd (and each even) path-spiral is higher than the previous one.

Each ion reflected from its path end $\rho = 1$, spirals back along the same field line. But after a collision the ion spirals along a nearby field line.

The magnetic energy must substantially exceed the kinetic energy. Only in this case is the magnetic field frozen in the plasma, and the magnetic field lines go through the guiding centers of the particle paths. If this condition is no longer fulfilled, the particles' orbits are more complex, and they can escape.

4. TOP-TRAPPING: THE UPWARD DIFFUSION OF THE HIGH-ENERGY PLASMA ($E_{(1)} < 1$) IN UNDISTURBED ATMOSPHERES ($n = 3$)

Trajectories of ions, spiraling either in disturbed or undisturbed atmospheres, are pictured in Figure 1 for the various $E_{(1)}$ and n. The uppermost two spirals refer to stationary, dipole-like atmospheres and these two paths are reproduced in detail in Figure 2. The upper path of Figure 2, belonging to superescape charged particles ($E < 1, v > v_{esc}$) already contains a slight indication of top-trapping: Follow how the pitch angle i and the altitude differences $d\rho \propto \cos i$ vary when the particle spirals away from its path end $r_{(1)}$, which is the magnetic mirror r_H. At $r_{(1)}$, where $i = 90°$, dr is theoretically zero. At higher altitudes, where the path rises, the pitch angle i continuously diminishes and, consequently, the altitude difference, $dr/dt \sim \cos i$, passed through during equal time intervals, continuously grows.

Consequently, charged particles which begin their path with the same velocity and the same pitch angle surmount longer altitude differences dr/dt if they are moving upwards than if they are moving downwards. See Figure 3 where each path begins with $i = 60°$.

The process of top-trapping is perhaps best explained if we define a mean ion that after successive energy-conserving collisions always (1) alternatively spirals up and down along the same field line H, and (2) begins its new path with the same pitch angle i, say, $i = 60°$.

Figure 3 shows the trajectory of such a mean superescape charged particle after three collisions. The particles gradually diffuse upwards. The equilibrium distribution of particles with $v > v_{esc}$ fills the magnetosphere.

For example, a stationary cosmic atmosphere drawn at the left edge of Figure 4 is evidently filled with the top-trapped superescape charged particles spiraling with $v > v_{esc}$; see Woyk (1968).

This also explains why violent bursts of plasma from below the solar photosphere turn into stationary prominences often living weeks (more than one solar rotation). Their dense tops hover motionless in the atmosphere, apparently without any contact with the photosphere. When the kinetic energy of the prominence attains the magnetic energy the prominence often bursts into pieces like a rigid arc.

5. GRAVITOMAGNETIC EXPLANATION OF CLOSE BINARIES

In close binaries, one stellar component pours plasma from its accretion disk on the other star; see Figure 5. Assume the accretion disk of the primary stellar component is just the top-trapped high-energy belt hovering above the magnetic equator. This accretion disk is continulusly filled with the high-

FIG. 4.—Three typical gravitomagnetic cosmic atmospheres: *left*: filled with superescape particles (one equatorial ring); *center*: underescape ions prevail (two side-trapped rings); *right*: the plasma burst from the stellar core—H is not strong enough, and the axis of rotation differs from the magnetic one.

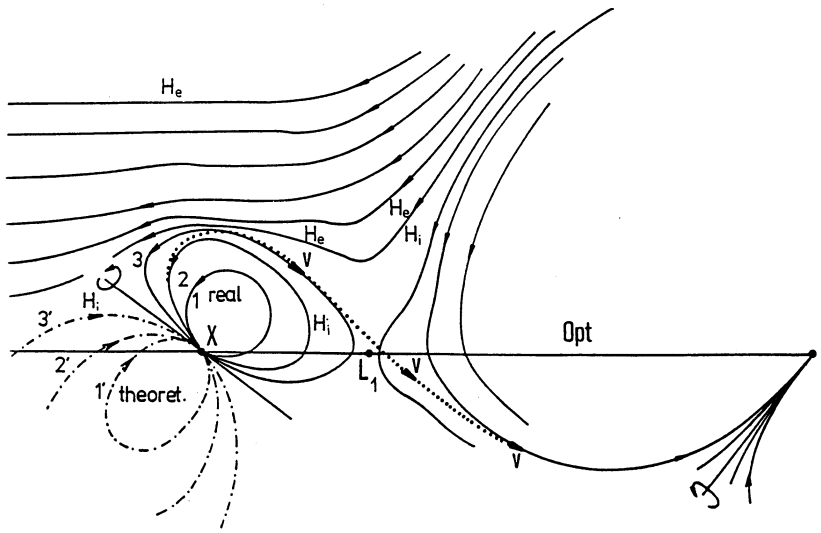

FIG. 5.—Gravitomagnetic model of close binaries. *Solid lines*: magnetic field lines H_i are inside the star, H_e in the external space. The dotted line roughly reproduces the path spiral which propagates from one stellar component to the other one through L_1.

energy charged particles that still spring up from the star and become top-trapped (so that they cannot reenter the inner star). No escape in any other direction is possible. But, so as their number grows, the kinetic energy density of the plasma approaches the magnetic energy density. Consequently the ions slowly start spiraling along higher and higher field lines as indicated by the dotted line v in Figure 5. However, the magnetic field of the external space, H_e, which had been squeezed by its deviation along the star, is stronger. Thus, in equilibrium also H_i grows near the top. The inner magnetic field H_i is still strong enough to impede an immediate escape of the almost horizontally flowing top plasma. Thus, after having attained and passed the top of the field lines, the plasma cannot yet escape outwards. It attains the empty space round the libration center L_1, and it streams straight forward on the other stellar component. As the primary component rotates, each field line continuously pours a part of its plasma surplus through L_1 on the magnetic field of the secondary star.

A preliminary discussion was given by Woyk (1967, 1972).

6. CONCLUSIONS

This paper deals with stationary undisturbed atmospheres only, characterized by $n = 3$. The top-trapping, that is, the upward diffusion of superescape charged particles ($v > v_{esc}$, or $E < 1$) explains the extremely high temperature at the tops of very high magnetic field lines in solar and stellar coronae and prominences, planetary radiation belts, planetary nebulae (Woyk 1968), close binaries, etc. Slower, underescape charged particles ($E > 1$) cannot be top-trapped. At best they are side-trapped (Fig. 2). A subsequent paper will treat disturbed media ($n \neq 3$) with a variable value of n.

REFERENCES

Woyk, E. 1967, Atm. Terr. Phys., 29, 465
———. 1968, in IAU Symp. 34, Planetary Nebulae, ed. D. E. Osterbrock & C. R. O'Dell (Dordrecht: Reidel), 275
Woyk, E. 1972, Bull. Astron. Inst. Czechoslovakia, 23, 278